Available online at www.sciencedirect.com
SCIENCE DIRECT®
Earth and Planetary Science Letters 239 (2005) 79–97
EPSL
www.elsevier.com/locate/epsl

Revisiting the rare earth elements in foraminiferal tests

Brian A. Haley [a,*], Gary P. Klinkhammer [b], Alan C. Mix [b]

[a] Department of Earth Sciences, University of Bristol, Wills Memorial Building, Queen's Rd., Bristol BS8 1RJ, United Kingdom
[b] College of Oceanic and Atmospheric Sciences, Oregon State University, 104 Ocean Admin. Bldg., Corvallis, OR, 97331, United States of America

Received 8 December 2004; received in revised form 24 August 2005; accepted 25 August 2005
Available online 28 September 2005
Editor: E. Boyle

Abstract

Are the rare earth elements (REEs) in foraminifera a valuable proxy for use in paleoceanographic and climate change studies? In order to investigate this, we attempted a comprehensive study of REEs in planktonic and benthic foraminifera. Several different cleaning protocols were tested. Although the hydroxylamine used to clean all foraminifera in this study removes an unidentified source of REE contamination, it seems to remobilize metal oxides that are otherwise unaffected in flow-through dissolution. The calculated REE distribution coefficients, $K_{D(REE)}$s, are between 100 and 500 for both planktonic and benthic foraminifera. These K_Ds are high compared to other elements in biogenic calcite but can be explained through a general model of element incorporation during foraminiferal calcification.

From data taken from eight core tops in the southeast Pacific, we conclude that the REEs in planktonic foraminifera are, indeed, useful as a proxy for upper ocean water mass and mixed layer biogenic productivity. Alternatively, the REEs in benthic foraminifera are useful as a proxy for carbon flux to the sea floor. These proxies should be robust down core unless the sediments have undergone anoxic diagenesis, which stabilizes Fe carbonate thus overprinting the primary REE signature. However, it is clear from REE distributions in foraminiferal tests if anoxic conditions have occurred.
© 2005 Elsevier B.V. All rights reserved.

Keywords: rare earth elements; foraminifera; paleoceanography; geochemical; indicators; southeast pacific

1. Introduction

There is an increasing demand for a wider arsenal of geochemical proxies to investigate paleoceanographic and paleoclimatic change. This need is reflected in the number of such investigations (e.g., [1–11]). With more and better estimates of temporal and spatial changes in oceanic characteristics, we should gain a better understanding of the ocean's role in climate change. The challenge is to develop proxies of oceanic properties that are both accurate and reliably preserved in the geologic record of marine sediments.

Over twenty years ago the rare earth elements (REEs) were recognized for having potential for paleoceanographic studies [12] but two issues have hindered their utilization. First, there was a lack of understanding of the behavior of REEs in the diagenetic environment (marine pore water), which precluded estimating alteration of the primary foraminiferal signal. Second, the cleaning procedures typically used to remove contaminant phases (e.g., [13]) were subject to the effects of REE readsorption, a challenging characteristic of these elements [14].

* Corresponding author. Current address: IFM-GEOMAR, East Shore Campus, Wishhofstrasse 1-3, 24148 Kiel, Germany. Tel.: +49 431 600 2252; fax: +49 431 600 2925.
E-mail address: bhaley@ifm-geomar.de (B.A. Haley).

0012-821X/$ - see front matter © 2005 Elsevier B.V. All rights reserved.
doi:10.1016/j.epsl.2005.08.014

These two issues have now been addressed [15,16], which allows us to revisit the potential of making paleoceanographic reconstructions based on REEs in foraminiferal calcite. This process of establishing a robust paleoproxy has two facets: First, the proxy must be understood in light of the modern ocean and subsequent diagenetic influences; second, the proxy must be assessed over time in light of other paleoceanographic data (e.g., $\delta^{18}O$; $\delta^{13}C$). Both of these aspects of proxy development are critical in that without one, interpretations of the other are weakened. Hence, given the importance of both these investigations to the future of the potential proxy, it is important that each is treated individually in a comprehensive way. Our goal here was to determine if REEs reflect, in a predictable way, paleoceanographically useful aspects of the biogeochemistry of modern seawater and, if so, establish whether this signal is reliably preserved down core. That is, our aim was to fully investigate the "first aspect" of proxy development, leaving the latter test of the proxy over time for a future study. In addressing this objective, we followed two lines of investigation: a study of foraminifera in core tops recovered along the southeast Pacific margin and a down core comparison of REEs in foraminifera from oxic and anoxic sedimentary (diagenetic) environments.

From the results presented here, we conclude that REEs in planktonic foraminifera do reflect water mass characteristics, and will be useful as a proxy for sea surface biologic productivity and for tracing upper ocean circulation. Benthic foraminiferal REEs appear to be a good proxy for carbon flux to the sea floor (i.e., export production). These results can be mechanistically explained from a current understanding of REE behavior in the oceans and pore waters (e.g., [16,17]). However, we also show that intense diagenesis can overprint the primary planktonic or benthic REE signals. Fortunately, such overprinting is easily detected by its diagnostic REE characteristics and this information too may be useful for paleoceanographic interpretation.

2. Methods

2.1. Samples

Foraminifera were handpicked from the >125 μm size fraction of core top (<2 cm depth sections) sediment from multicores collected at 8 sites along the Chile margin and at one site off Central California, all archived at the Oregon State University Marine Geology Core Repository (Fig. 1; Table 1). In addition, down core samples were taken from 5 depth intervals at Sta. 10 and 54MC. The number of foraminifera obtained depended upon availability and size of the individuals in each sample. We selected 10 to 15 shells

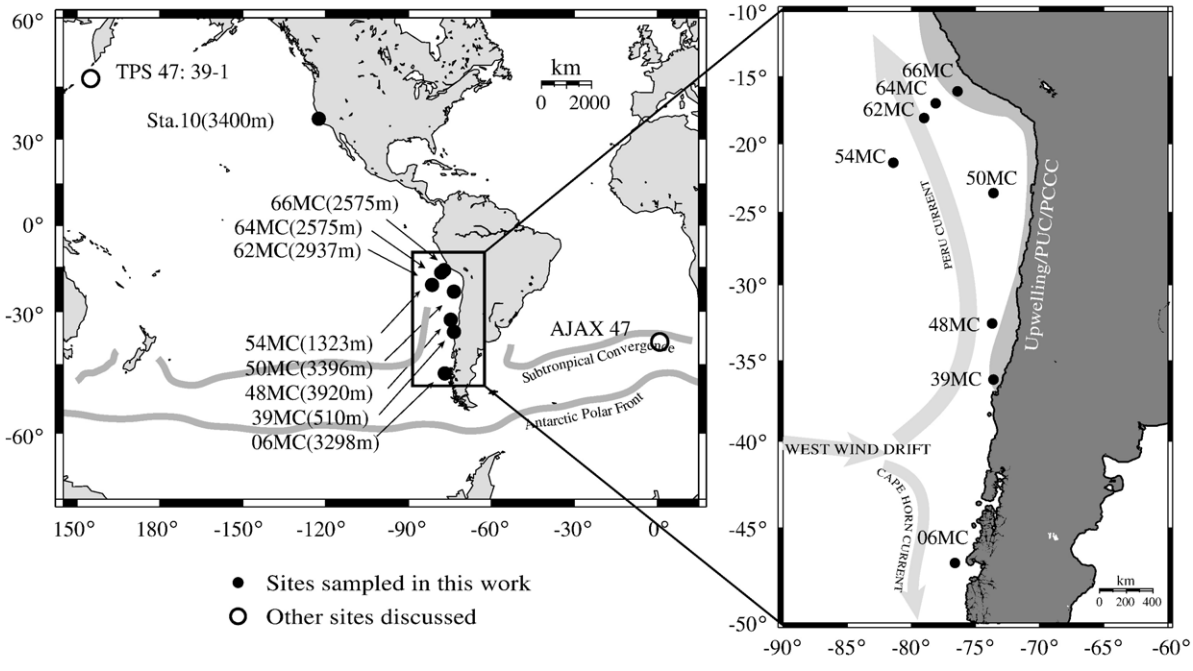

Fig. 1. Site locations. Selected ocean currents and boundaries shown in gray. Box in right-map shows area enlarged in left-map.

Table 1
Site descriptions

Site	Latitude	Longitude	Depth (m)	Estimated primary productivity (g cm^{-2} y^{-1})[a]	Bottom water oxygen (μM)
ME 00005A-06MC	46° 53.00 S	76° 36.00 W	3298	71	NDA[b] (185)[c]
ME 00005A-39MC	36° 10.03 S	73° 34.28 W	510	201	63 (167)
ME 00005A-48MC	32° 35.45 S	73° 39.10 W	3920	120	NDA (170)
ME 00005A-50MC	23° 36.38 S	73° 36.45 W	3396	100	160 (165)
ME 00005A-54MC	21° 21.56 S	81° 26.13 W	1323	72	104 (143)
ME 00005A-62MC	18° 05.80 S	79° 02.40 W	2937	105	149 (154)
ME 00005A-64MC	17° 02.12 S	78° 06.53 W	2930	139	150 (156)
ME 00005A-66MC	16° 07.61 S	77° 05.89 W	2575	213	150 (147)
Sta. 10	36° 06.11 N	122° 35.23 W	3400	238	128 (76)

[a] Estimates from Antoine et al. [61,62].
[b] NDA = No data available.
[c] Data in parentheses is World Ocean Atlas data estimate [60]. The discrepancy of these estimates, compared to the measured values, precludes using them in REE data interpretation.

of benthic foraminifera (mono-specific) and 20 to 30 shells of planktonic foraminifera (mono-specific where possible). We attempted to choose the benthic species *Cibicidoides wuellerstorfi*, *Uvigerinidae peregrina* and *Globobulimina affinis* as representatives of epifaunal, shallow infaunal and deep infaunal habitats, respectively, at each site. This was, however, not always possible. In particular, oxic sedimentary environments had too few (if any) *Globobulimina* present, thus precluding analyses of foraminifera from deep infaunal habitats in oxic environments.

2.2. Sample preparation

It is often assumed that in order to evaluate the trace element content of primary biogenic calcite it is necessary to physically and chemically clean the foraminifera shells, removing contaminant phases (e.g., [13,18]). While the traditional cleaning methods face problems of readsorption when cleaning for REEs [14], use of a "flow-through" (FT) system has the potential for overcoming, or at least minimizing, such problems [15]. Klinkhammer et al. [19] describe the FT-system used in this study, in which the foraminifera are not physically cleaned (i.e., no cracking, sonification or rinsing) and are loaded directly into small dead-volume sample "cartridges" (1 μm mesh Teflon syringe filters) without any pretreatment. Minor element distributions appear to be more consistently replicated, less influenced by contamination, and the primary calcite better separated from contamination using this methodology [19]. However, because trace elements in foraminiferal calcite are more sensitive to contamination than minor elements, the influence of contaminant phases must be rigorously evaluated, especially for REEs which tend to readsorb [14].

Three different cleaning experiments were run, each using a sample of planktonic foraminifera from the oxic sediments of site 54MC: (1) only a DIW-rinse was done (DIW was used as the "cleaning" solution); (2) cleaning was done with hydroxylamine (HYDRX, at pH=~9), to remove metal oxide phases; (3) cleaning was done with diethylene triamine pentaacetic acid (DTPA, at pH=~9), to remove a refractory phase that is probably barite [20,15,21]. In order to determine the effectiveness of each of these treatments individually in removing potential contaminant phases we did not apply multiple cleaning steps. The results of these cleaning experiments are summarized in Fig. 2.

In general, the La:Ca ratios are consistently low (<0.1 μmol:mol) at the onset of dissolution (in 4 mM HNO_3) and increase during more rapid dissolution at the end of the experiment (in 10 mM HNO_3). This increase in La:Ca is ~4-fold for the DIW and DTPA-cleaned sample but only ~2-fold for the HYDRX-cleaned sample. Beyond this change (seen in each experiment), the REE:Ca differed between all three cleaning methods. These REE:Ca observations can be compared to the Fe-, Mn- and Ba:Ca ratios from each experiment; the latter are similar both throughout the dissolution and in comparison to each other for both the DIW- and DTPA-cleaned experiments, but are significantly higher in the HYDRX-cleaned sample (note logarithmic scale for Mn:Ca in Fig. 2).

We envision three possible explanations for these REE and trace element behaviors observed during flow-through dissolution: (1) The REEs are readsorbed back onto the calcite, even as the calcite slowly dissolves in the weak acid; (2) the foraminiferal calcite itself is heterogeneous with respect to REEs, but not for Fe, Mn or Ba; (3) there is a REE-enriched (but Fe-, Mn-, Ba-depleted) contami-

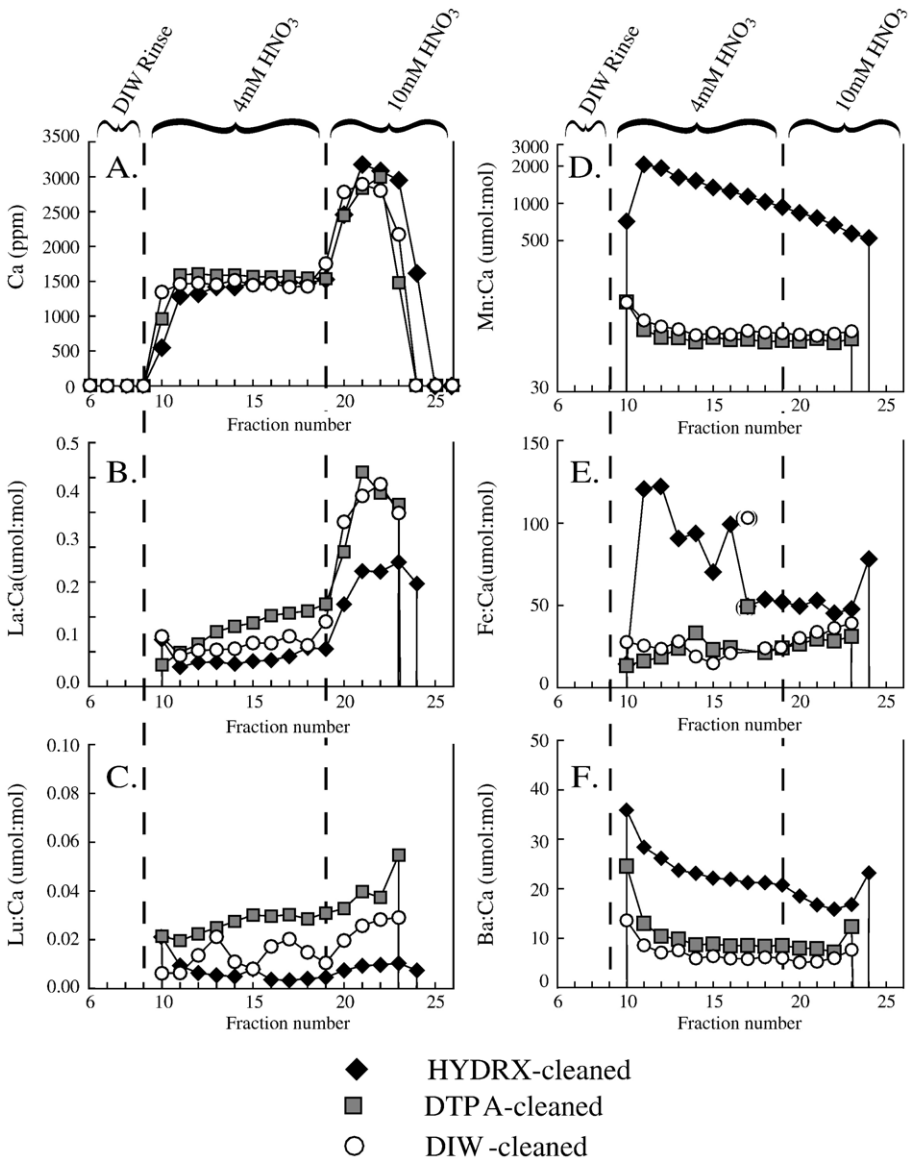

Fig. 2. Calcium and element : calcium ratios in the final step-wise dissolution phase of foraminifera from three cleaning experiments: (1) hydroxylamine (HYDRX) cleaning; (2) diethylene triamine pentaacetic acid (DTPA) cleaning; (3) simple DIW-rinse. Nitric acid concentration, during the dissolution (tubes 9 through 24) has a step-function, whereby the concentration is held constant at 4 mM (tube 1 through 18), then increased to 10 mM (tube 19 through 26). Tubes 6 through 9 are collected during the system rinse: elemental concentrations are below detection in these fractions. Leaching of clay was monitored by measuring Al, but remained insignificant throughout each experiment. A: Ca-concentration indicating each experiment had similar general dissolution characteristics. B and C: La : Ca and Lu : Ca (lightest and heaviest REE : Ca, respectively) measured during dissolution. The lowest REE : Ca ratios are seen in the HYDRX-cleaned experiment, suggesting that HYDRX removes a source of REE contamination. D, E and F : Mn : Ca, Fe : Ca and Ba : Ca in each fraction collected. These element : Ca ratios may be affected most significantly by the contaminant phases Mn-oxide, Fe-oxide and barite, respectively. The elevated ratios in the HYRX-cleaning experiment suggest Mn-oxides are being remobilized, but not completely removed, by the HYDRX.

nant phase that is somewhat eroded by DIW and more so by the HYDRX (Fig. 2).

To assess the first possibility, that the REEs are readsorbing, we tested whether a simple readsorption model (see Appendix) could reproduce the observations shown in Fig. 2. For each experiment the model could reproduce the REE : Ca dissolution variation quite well, from a single REE : Ca ratio (considered the true signal) and a defined set of "readsorption coefficients" (Fig. 3). These coefficients prove to be remarkably high (up to 60% for the 4 mM HNO_3 that follows cleaning). Although in previous work [15] we saw no signs of

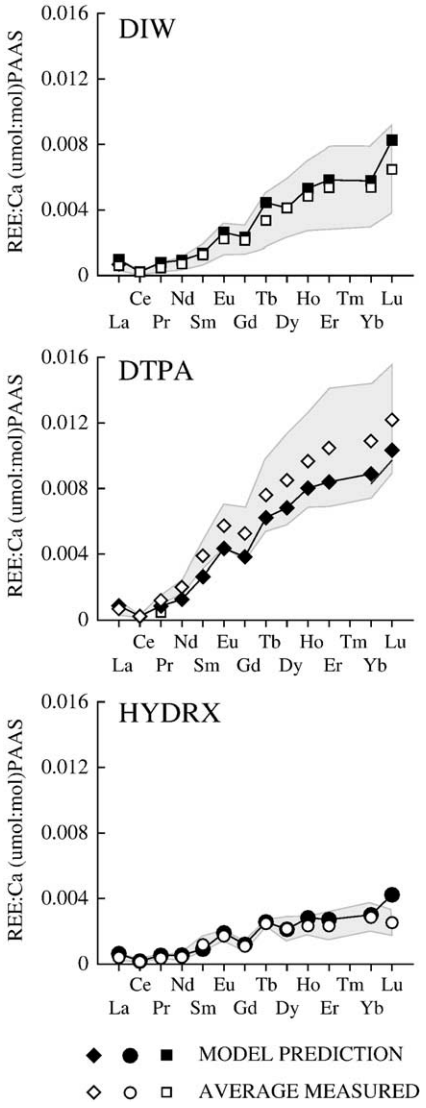

Fig. 3. Model predicted (solid) and measured (open) REE patterns from cleaning experiments. The gray envelopes around the measured values indicate the range of REE values (normalized) found for each experiment during the final dissolutions. In general, the HYDRX-cleaned sample has the lowest REE concentrations measured, the DTPA-cleaned sample has the highest. In all three experiments, however, the REE pattern is "seawater-like." The readsorption model predictions are similar to the mean measured value, especially for the HYDRX-cleaned experiment, suggesting that the mean value is a good approximation for the original primary calcite REE:Ca ratio.

readsorption, the current method dissolves foraminiferal shells much less aggressively (using 4 and 10 mM HNO_3 versus 50 mM HNO_3). It is most likely that in this current method the pH within the system (especially in the 4 mM HNO_3) is not low enough to fully prevent readsorption. This implies that the REEs can adsorb with remarkable efficiency (particularly the LREEs, which always have higher "readsorption coefficients" than the HREEs), especially given that the pH of these fractions was less than 7 in all fractions. For paleoproxy purposes, the important point is that the REE-dissolution profiles (Fig. 2) can be modeled with a single REE:Ca ratio, which is similar to the Ca-weighted-average pattern measured (Fig. 3), which suggests that the variations in REE:Ca may be due to readsorption alone.

Another idea to explain the varying REE:Ca values observed (Fig. 2) is that the calcite itself has heterogeneous REE:Ca. Foraminiferal calcite is heterogeneous in many respects, both physically [22,23] and chemically [24–27], and it seems likely that REEs might be heterogeneously distributed as well [15]. To judge whether heterogeneity is more important than readsorption in creating the variable REE:Ca observed during each experiment, we ran an inorganic, homogenous calcite ("Wiley" marble: a marble that is ~100% calcite and homogenous optically, for $\delta^{18}O$, for $\delta^{13}C$ and for minor element:Ca ratios; [19]; unpublished results). Again, the REE:Ca dissolution profile showed variability (not shown) that was possible to reproduce with the readsorption model. This suggests that, even if the shell is heterogeneous, readsorption is the dominant reason for the variable REE:Ca observed through time (Fig. 2).

While readsorption may explain the variation of REE:Ca within each experiment, it does not necessarily explain the differences between the three cleaning methods. Although a REE-enriched contaminant phase would seem the most likely explanation for the overall differences in REE concentrations between these cleaning experiments, the observations are not as straightforward. That is, the REE:Ca content of the "cleaned foraminifera" in these experiments follow the trend: HYDRX<DIW<DTPA, whereas the Fe-, Mn- and Ba:Ca ratios follow the trend: HYDRX>DIW=DTPA (Fig. 2).

Our inference of the latter trend is that the HYDRX remobilizes, but does not completely remove, metal-oxide coatings, such that they become prone to mobilization during the acid dissolution. If so, the REE content can only be lowest after HYDRX-treatment if (1) Mn-oxide has insignificant REE content [15,16,28], and (2) HYDRX-cleaning removes another, undetermined source of REEs.

By using increasingly dilute acids during the dissolution, the influence of barite is circumvented, as is suggested by the similarity between the DIW- and DTPA-cleaned experiments. That is, although barite could be removed through the use of DTPA, barite is

not prone to mobilization during dilute acid dissolution (Fig. 2; [29,30]) even for DIW-cleaned shells. Likewise, clay cannot be a factor as we do not see Al in any fraction measured (being chemically separated, as discussed in [19]), nor do the REE patterns (Fig. 3) indicate clay contamination (flat patterns normalized to the Post-Achaean Australian Shale–PAAS-composite; [31]).

Although more work needs to be done to resolve the influence of contamination on foraminiferal REEs, it is important to first establish that such an effort would be profitable: that is, that there is potential of using REEs as a paleoproxy. Such an evaluation follows, through analyses of core top foraminiferal samples. We chose to clean these samples with HYDRX, even with reservations about the apparent remobilization of metal-oxide phases, because it can be argued that the lowest REE:Ca ratios are likely to be the least potentially contaminated, an argument that is not necessarily valid or accurate, but widely accepted. As discussed above, DTPA was not used as a cleaning step, because our dissolution scheme does not appear to affect barite.

The cleaning procedure ultimately used for the samples reported in the Results section is outlined in Table 2 (for details of the FT cleaning system and reagents used, see [15]). Discrete fractions were collected by the fraction collector every 2 min (4 mL samples) and only during the acid dissolution phase.

Table 2
Cleaning protocol

Time (min)[b]	% Reagent at each time step[a]			Event
	0.5 M HYDRX	10 mM HNO_3	DIW	
0.0	0	0	100	
1.0	100	0	0	Cleaning
6.0	0	0	100	
10.0	0	0	100	
10.1[c]	0	50	50	System rinse
12.0	0	50	50	
15.0	0	0	100	
17.0[d]	0	0	100	Sample rinse
20.0	0	0	100	
21.0	0	40	60	"Weak acid" sample dissolution
30.0	0	40	60	
31.0	0	100	0	"Strong acid" sample dissolution
47.0	0	100	0	
48.0	0	0	100	Reset system

[a] A constant gradient was generated between each programmed time step.
[b] Flow rate is 2 mL/min throughout the cleaning and dissolution.
[c] Valve switch bypassing sample.
[d] Valve switch return flow to sample.

2.3. Mass spectrometry

The fractions collected were measured on a VG Axiom High Resolution Inductively Coupled Plasma Mass Spectrometer (HR-ICP-MS) at the Keck Collaboratory at Oregon State University. The REEs and Ba were analyzed at low resolution (400 RP) to optimize detection sensitivity and measure significant counts-per-second (CPS) on each of the trace-abundant REE isotopes. This is not ideal since the REEs are prone to molecular interferences in the ICP-MS. To reduce this problem, oxide formation was kept to a minimum by adjusting torch position and gas flows in the plasma (typically <5% of CeO formation as seen at 156 Gd compared to 140 Ce). The isotopes 46 and 48 Ca, 186 27 Al, 55 Mn and 56 Fe were analyzed at high resolution (7000 RP) to either reduce the ion beam (in the case of Ca and Al) or for resolution purposes (for Fe and Mn). No internal standard was used, as this increased the potential for contamination of the already weak REE signal. Instead, several (4 to 10) replicates of 2000- to 4000-fold dilute PPREE and SCREE ("Paradise Portal REE"; "Spring Creek REE") standards were measured over the course of each analytical run to verify the standard curve consistency. These PPREE and SCREE standards are diluted mine-waste contaminated river waters (see [32] and [33]), and their replicated analyses indicate that typical accuracy is ~5% for these analytes.

3. Results

3.1. Distribution coefficients of the REEs in foraminiferal calcite

Published REE:Ca in foraminiferal calcite predict apparent distribution coefficients (K_Ds) that may seem unreasonably high, suggesting that the samples are contaminated [6,12,34]. This has been the source of significant consternation over the applicability of a REE paleoproxy, as such an inference would compromise the validity of core top and down core data. Therefore, the REE K_Ds in foraminifera warrant brief discussion.

The substrate composition used for the K_D calculation is critical (surface seawater for planktonic foraminifera; overlying bottom water for epifaunal benthic foraminifera; pore water for infaunal benthic foraminifera). Fortunately, the calculation done here uses the REE concentrations in overlying and pore water measured in the same core from which the benthic foraminifera were obtained (64MC; Table 3). Unfortunately,

Table 3
Distribution coefficients of REE in foraminiferal calcite

REE : Ca[a]	La	Ce	Pr	Nd	Sm	Eu	Gd	Tb	Dy	Ho	Er	Tm[b]	Yb	Lu
Foraminifera model result[c]														
N. dutertrei (planktonic)	0.86	0.34	0.16	0.65	0.12	0.04	0.17	0.03	0.21	0.04	0.14	*0.04*	0.12	0.02
Cibicidoides (epifaunal benthic)	0.99	0.74	0.19	0.69	0.17	0.05	0.20	0.02	0.28	0.05	0.20	*0.06*	0.16	0.02
Uvigerinidae (infaunal benthic)	4.49	2.71	0.84	3.66	0.63	0.22	0.83	0.14	0.97	0.20	0.66	*0.19*	0.62	0.09
Surface water														
AJAX 47[d]	1.09	0.54	NA	0.79	0.15	0.04	0.24	NA	0.29	NA	0.28	NA	0.23	0.04
TPS 47: 39-1[e]	1.76	0.59	NA	1.22	0.23	0.06	0.34	NA	0.39	NA	0.35	NA	0.31	0.05
64MC[f]														
Overlying water	4.84	0.89	0.64	2.74	0.41	0.15	0.57	0.11	0.89	0.22	0.87	0.12	1.04	0.18
Pore water (0.21 cm depth)	12.2	2.67	2.34	9.08	2.11	0.60	3.00	0.55	4.15	0.93	3.37	0.62	4.70	1.00
K_D[g]														
N. dutertrei (AJAX)	790	630	–	820	830	1010	680	–	730	–	480	–	535	535
N. dutertrei (TPS 47: 39-1)	490	580	–	535	530	650	490	–	530	–	390	–	400	350
Cibicidoides (overlying water)	205	830	295	250	420	310	345	215	315	220	230	*470*	150	120
Uvigerinidae (pore water)	370	1020	360	405	300	370	280	250	235	215	195	*310*	130	95

[a] Foraminiferal data in μmol:mol units; seawater and pore water data in nmol:mol units, assuming 10.46 mmol/L Ca for all seawater and pore water.
[b] The foraminiferal Tm data are suspect, probably due to inter-REE molecular interferences in the ICP-MS.
[c] Foraminifera from core top (0–2 cm section) of 64MC multicore.
[d] Average 0–200 m depth water samples from German et al. [35].
[e] Average 0–200 m depth water samples from Piepgras and Jacobsen [37].
[f] From Haley et al. [16].
[g] K_D values rounded to nearest 5.

there are few surface seawater REE data, especially in the southeastern Pacific. Exacerbating this, the uncertainties associated with aeolian input and short upper ocean residence times make comparison of planktonic foraminiferal REEs to any water mass other than the one from which the calcite precipitated prone to errors. However, in light of the precisions we are concerned with in making these K_D calculations, an approximate surface seawater REE composition should be acceptable. In Table 3, we offer two possible candidates (Fig. 1): (1) surface water from the southern Atlantic (AJAX data from [35]), that might be similar to 64MC provided that both sites reflect upwelling of Antarctic Intermediate Water (AAIW), and; (2) Northern Pacific surface water, probably a poor choice as these data should reflect North Pacific Intermediate Water (NPIC; [36]; REE data from site TPS 47: 39-1 of [37]).

As shown in Table 3, the REE K_D is estimated to be ~100 to ~500 (excluding Ce). Considering the potential errors in making these calculations, we argue that these K_D values are accurate. The consistency of the K_Ds (1) across the REE series, and (2) considering the dramatic differences in REE content of the water in which these foraminifera live, supports these K_D estimates. For example, pore water REEs are typically an order-of-magnitude more concentrated than surface water REEs but the K_Ds calculated are similar. K_D(Ce) is anomalously high, which may be an artifact but could equally well result from Ce being in a different redox state compared to the other REEs.

These estimates of K_D are contrary to those of Pomies et al. [6] (from Nd isotopes), but consistent with previous REE observations [15] and the Nd-isotopic data of Vance and Burton [38,39]. Nonetheless, if these K_D values are accurate, it follows that the foraminifera preferentially incorporate REE relative to Ca into their shells! Since there is no currently known biologic requirement for REEs, this preference seems unlikely. However, there are other possible explanations for such high K_Ds. For example, Palmer [12] argued that the solubility product of REE carbonates plays a role in establishing high K_Ds. Alternatively, Lakshtanov and Stipp [40] have measured K_D(Eu) >700 for inorganically precipitated calcite, which they attribute to the ability of Eu to fit into the calcite lattice as a true solid solution.

We suggest that the relatively high concentration of REEs in foraminiferal calcite is a consequence of the organic chemistry of calcite precipitation. Our speculation is that REEs, which are known to have great affinity to organic matter [e.g., 28,41–47], preferentially bind to the proteins used by the foraminifera to acquire calcium ions to build their shells [48]. Thus, there are elevated levels of REE associated with these biomolecular agents of calcification (relative to REE and Ca in seawater), and the shell is made with an

"anomalously" high REE content. In this scenario, the relative enrichment of any ion in the calcite will depend on both the concentration of the ion in seawater and the binding efficiency of that ion with the protein.

Although we cannot test this hypothesis, Fig. 4 attempts to show that it is not unreasonable. Fig. 4 shows that the K_Ds of trace elements, minor elements and even calcium ($K_D=1$) are positively correlated with the stability constant of that ion, for three amines (a primary amine and two tertiary amines), for which there are published $K_{stab.}$ and K_D data. Estimates for these values are from the compilations of Lea [49] and Martell and Smith [50]. Regardless of the mechanism, we consider that the observed K_Ds, up to ~500, are accurate. Assuming this is correct, we now present the core top sampling results that are used to determine if, and how, the REEs might serve as a useful paleoproxy.

3.2. Core top samples

The core top foraminiferal REE:Ca data are presented in Table 4 and shown in Fig. 5. The data are grouped according to living habitat: planktonics in the upper water column; *Cibicidoides* at the sediment–water interface (epifaunal); *Uvigerinidae* just below the sediment–water interface (shallow infaunal); *Globobulimina* and *Bulimina* deeper in the sediments (deep infaunal). Although there is currently some debate over the exact habitats of these foraminifera [51], these divisions are used here to reflect the foraminifera's apparent preference for a given diagenetic environment.

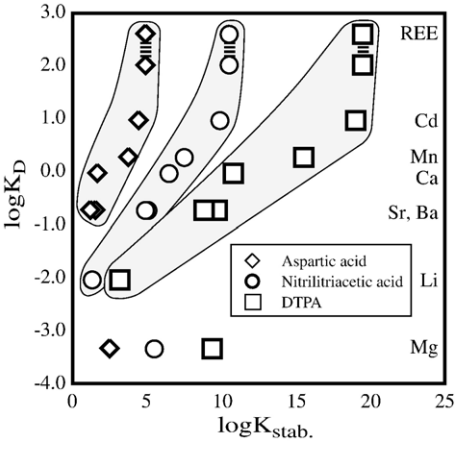

Fig. 4. K_D versus log $K_{stab.}$ for three amines. The positive relationship shown suggests that metal complexation with proteins might explain the high apparent K_Ds observed from foraminiferal shell analyses. The fact that Mg does not fit with these trends may indicate that Mg incorporation into foraminiferal calcite is more strictly regulated during biomineralization than other elements. Data are from Lea [49] and Martell and Smith [50].

That is, "deep benthic" species may be found shallow in a core having high organic carbon content that reaches anoxic conditions at a shallow depth. Likewise, "deep benthic" species may not be found at all in cores that remain oxic throughout their depth.

3.2.1. Planktonics

Except at Sta. 10, the planktonics show a shale-normalized pattern similar to typical seawater (Fig. 5; Table 4): i.e., HREE>LREE, with a pronounced negative "Ce anomaly" [17,52]. Only the sample from Sta. 10 shows signs of a middle REE (MREE) enrichment relative to a linear trend from the LREEs to HREEs (MREE*=1.59; HREE:LREE=~1). Sta. 10 is also the most overall REE-enriched, although 06MC is nearly as concentrated. 66MC and 54MC samples have the least REE abundance and share similar patterns, although the HREEs at 54MC are higher than those at 66MC (Fig. 5). In fact, 54MC has the steepest sloped pattern of all these sites, with a HREE:LREE of 6.08. 64MC and 48MC are similar in both pattern and abundance of REEs, as are 62MC with 50MC. The "Ce anomaly" of all these samples, except Sta. 10, 66MC and 06MC, ranges between ~0.25 to ~0.35. These three exceptions have higher "Ce anomalies" between 0.5 and 0.6. There do not appear to be any trend, either in concentration or pattern, dependent on species or mixed species.

3.2.2. Cibicidoides (epifaunal)

Although the abundance of REEs in the *Cibicidoides* samples is distinct (66MC>64MC, 50MC>54MC), the patterns are all fairly similar (Fig. 5): they are all seawater-like, although the slope (HREE:LREE) is greatest at 50MC (4.27), followed by 66MC (3.18), 64MC and 50MC (2.59 and 2.36; Table 4). None of the *Cibicidoides* show signs of MREE enrichment (MREE*<1.2 for all), and the "Ce anomaly" is similar to the planktonic counterpart at each site. The *Cibicidoides* "Ce anomalies" here are between ~0.2 and ~0.3 for all sites, except 66MC where the "Ce anomaly" is ~0.6.

3.2.3. Uvigerinidae (shallow infaunal)

The *Uvigerindae* can be split into three types: Sta. 10 and 06MC show a distinct "MREE-bulge" type pattern (MREE*>1.2); 39MC has a flat pattern (HREE:LREE=~1; MREE*=1.28; Ce*>~1); and the other samples are more similar to a seawater-type pattern (Fig. 5; Table 4). For these latter sites, the HREE:LREE, MREE* have similar values to the planktonics and *Cibicidoides* samples, although the "Ce anomalies" tend to be slightly higher (between

Table 4
REE:Ca in core top samples

Species[a]	Core	La[b]	Ce	Pr	Nd	Sm	Eu	Gd	Tb	Dy	Ho	Er	Tm[c]	Yb	Lu	HREE[d] / LREE	MREE*[e]	Ce*[f]
Mixed planktonic	Sta. 10	3.31	3.63	0.85	3.84	0.69	0.20	0.72	0.11	0.62	0.03	0.24	*0.01*	0.26	0.00	0.99	1.59	0.50
G. menardii/G. tumida	66MC	0.27	0.27	0.05	0.22	0.04	0.01	0.06	0.01	0.10	0.01	0.05	*0.00*	0.05	0.01	3.30	0.99	0.53
N. dutertrei	64MC	0.93	0.42	0.18	0.76	0.12	0.06	0.18	0.03	0.23	0.04	0.14	*0.05*	0.14	0.02	2.72	1.06	0.24
G. sacculifer	62MC	2.05	1.07	0.37	1.61	0.27	0.09	0.39	0.06	0.45	0.09	0.31	*0.08*	0.31	0.05	2.88	1.06	0.28
G. sacculifer	54MC	0.28	0.16	0.05	0.20	0.04	0.01	0.06	0.01	0.09	0.02	0.08	*0.03*	0.08	0.01	6.08	0.72	0.33
N. dutertrei	50MC	1.62	0.99	0.37	1.60	0.28	0.11	0.37	0.06	0.42	0.09	0.27	*0.05*	0.25	0.04	2.43	1.13	0.29
Mixed planktonic	48MC	1.01	0.57	0.27	1.10	0.22	0.08	0.24	0.04	0.27	0.05	0.15	*0.04*	0.12	0.01	1.79	1.25	0.25
Mixed planktonic	06MC	2.79	3.70	0.72	3.05	0.57	0.13	0.54	0.08	0.68	0.11	0.37	*0.11*	0.34	0.01	1.75	1.05	0.60
Cibicidoides	66MC	2.20	2.50	0.43	1.88	0.32	0.10	0.48	0.08	0.70	0.12	0.44	*BD*[7]	0.35	0.05	3.18	1.03	0.59
Cibicidoides	64MC	1.08	0.66	0.22	0.89	0.15	0.08	0.21	0.03	0.32	0.05	0.19	*BD*	0.13	0.02	2.59	1.09	0.31
Cibicidoides	54MC	0.44	0.17	0.07	0.33	0.06	0.02	0.08	0.01	0.11	0.03	0.09	*0.02*	0.09	0.02	4.27	0.84	0.22
Cibicidoides	50MC	1.41	0.66	0.29	1.21	0.23	0.08	0.28	0.05	0.33	0.06	0.20	*0.04*	0.19	0.02	2.36	1.18	0.23
Uvigerinidae	Sta. 10	6.34	10.35	1.75	6.95	1.35	0.33	1.36	0.21	1.17	0.19	0.54	*0.09*	0.43	0.05	1.00	1.54	0.71
Uvigerinidae	66MC	1.27	1.42	0.28	1.13	0.16	0.06	0.23	0.04	0.32	0.06	0.21	*0.05*	0.22	0.03	2.83	0.91	0.55
Uvigerinidae	64MC	1.17	0.75	0.23	0.98	0.16	0.06	0.22	0.04	0.26	0.05	0.18	*0.05*	0.18	0.02	2.72	1.05	0.33
Uvigerinidae	54MC	0.89	0.68	0.15	0.66	0.10	0.04	0.14	0.02	0.21	0.05	0.16	*0.04*	0.17	0.03	3.81	0.77	0.42
Uvigerinidae	50MC	1.64	0.69	0.38	1.65	0.29	0.09	0.36	0.06	0.43	0.08	0.27	*0.06*	0.27	0.04	2.45	1.09	0.20
Uvigerinidae	39MC	2.49	8.14	0.77	2.93	0.53	0.12	0.50	0.07	0.49	0.07	0.24	*0.05*	0.19	0.02	1.03	1.28	1.34
Uvigerinidae	06MC	5.27	9.13	1.50	5.79	1.14	0.31	1.14	0.18	1.15	0.20	0.60	*0.11*	0.49	0.05	1.34	1.32	0.74
Globobulimina	Sta. 10	8.77	16.50	2.39	9.66	1.84	0.49	1.83	0.28	1.57	0.25	0.71	*0.11*	0.55	0.06	0.94	1.56	0.83
Globobulimina	39MC	1.26	5.50	0.43	1.90	0.27	BD	0.27	0.02	0.45	0.00	0.10	*0.10*	0.15	BD	0.98	0.89	1.69
Bulimina	39MC	0.60	3.53	0.17	1.00	BD	BD	0.11	BD	0.31	BD	0.02	*0.06*	0.10	BD	1.04	0.51	2.52

[a] All samples from sediment sections 0 to 1 or 2 cm core depth.
[b] Values are REE:Ca in μmol:mol.
[c] Tm is suspect, probably due to inter-REE molecular interference in the ICP-MS.
[d] HREE:LREE is defined as the ratio of shale normalized averaged Er:Ca, Yb:Ca to averaged Pr:Ca, Nd:Ca.
[e] MREE* is defined as average shale normalized (Gd:Ca, Tb:Ca) divided by average (Pr:Ca, Nd:Ca, Er:Ca, Yb:Ca).
[f] Ce* is defined by 2(Ce:Ca)/(La:Ca+Pr:Ca), when all values are shale normalized.

~0.3 and ~0.6). Overall, the concentrations of REEs in these sample are similar to the *Cibicidoide*s, except the "MREE bulged" samples, which are 2- to 4-times more concentrated.

3.2.4. *Globobulimina and Bulimina (deep infaunal)*

These deeper dwelling foraminifera were found at just two sites: Sta. 10 and 39MC. Both of these sites are shallow and lie under highly productive surface seawater (Table 1). The REEs, however, are different between these sites (Fig. 5; Table 4); Sta. 10 has a distinct "MREE bulge" type pattern with high REE concentrations, whereas both species at 39MC show low REE concentrations and have flat patterns. The "Ce anomaly" is indistinct for all of these samples.

3.3. Down core samples

The purpose of developing any paleoproxy is to be able to make measurements down core, in order to infer oceanographic and climatic changes over time. The better a paleoproxy is understood, the more confidence can be imparted to those interpretations. A crucial aspect of this understanding is knowledge of any diagenetic changes that might influence the primary foraminiferal REE signal. Therefore, it is important to measure REEs in down core samples with the express goal of determining the impact of diagenesis or alteration. Although it is perhaps unsatisfying from a paleoceanographic standpoint, we feel it is unwise to make any paleoceanographic inferences until any potential diagenetic affects are understood.

With this in mind, 5 intervals were sampled from the top ~25 cm of two multicores: 54MC and Sta. 10. These two sites represent "end-members" in that 54MC is the most "open ocean" site (deep water, carbonate-rich sediments, with relatively low surface productivity and moderate bottom water oxygen; Table 1); and Sta. 10 represents a "margin" site (shallow near shore, clay-rich, with high surface productivity and suboxic bottom water; Table 1); these differences should be reflected in the diagenetic environments at these sites. Pore water data [16] delimit the diagenetic

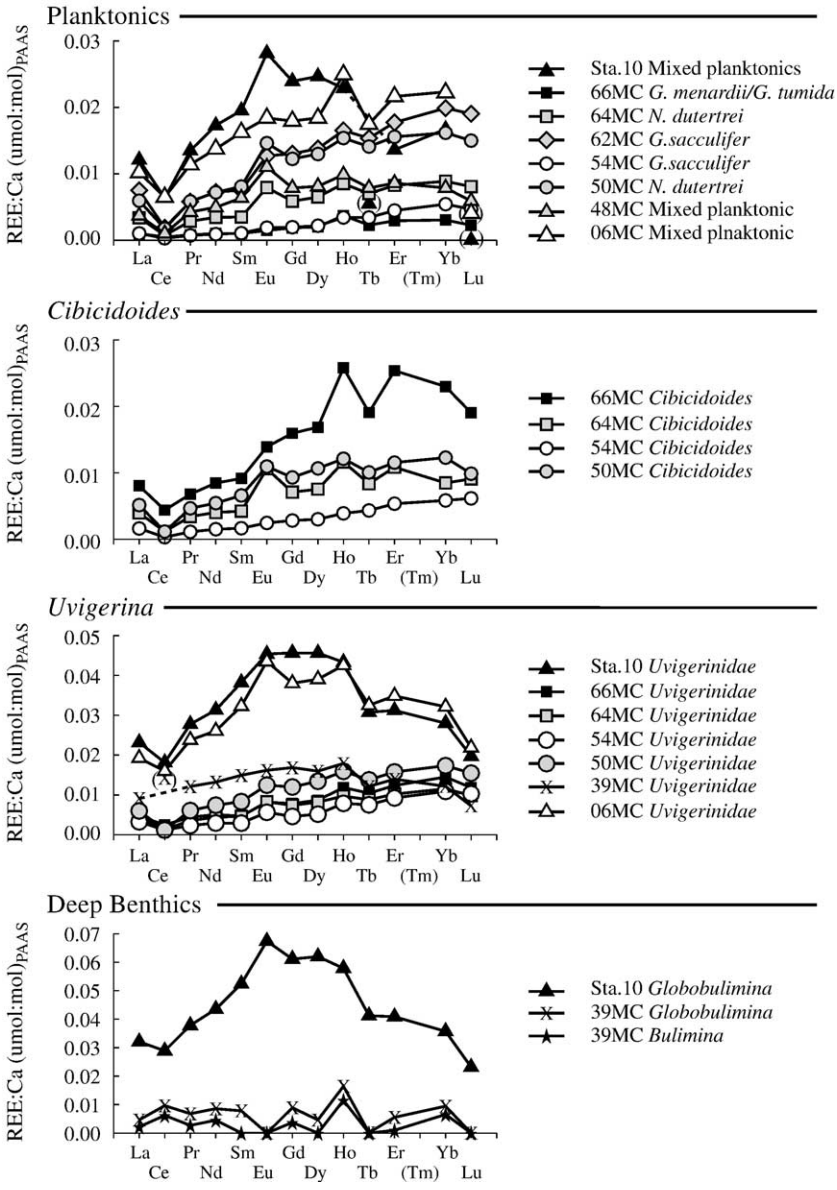

Fig. 5. Core top foraminiferal REE patterns. Grouped into typical living habitat (see text for details).

processes that influence REEs at these two sites. The foraminiferal data are listed in Tables 5 and 6 and shown in Fig. 6.

3.3.1. 54MC

This site is expected to have little diagenetic potential, being under an area of low surface productivity and having oxic pore waters (Table 1). The REE pore water profiles should be similar to the oxic sites of [16]; that is, with REE maxima at the sediment–water interface, generated from the remineralization of particulate organic carbon (POC).

REE patterns at 54MC all demonstrate a typical seawater form (Fig. 6), with remarkable consistency down core when comparing intra- and inter-species patterns. The HREE : LREE of the planktonics is between ~5.5 and ~6, slightly higher than the *Cibicidoides* (~4 to ~4.5) and the *Uvigerindae* (~3.5 to ~4). None of the patterns show signs of a MREE enrichment (MREE* < 1 for all samples), and the "Ce anomaly" is between ~0.2 and ~0.4 for all the samples. For every core depth, the *Uvigerindae* are more REE-concentrated than the *Cibicidoides* and both of these are more concentrated than the planktonics (Fig. 6).

Table 5
54MC down core REE:Ca ratios

Species	Depth(cm)	La[a]	Ce	Pr	Nd	Sm	Eu	Gd	Tb	Dy	Ho	Er	Tm[b]	Yb	Lu	HREE[c] / LREE	MREE*[d]	Ce*[e]
G. sacculifer (unclean)	0–2	0.51	0.29	0.10	0.41	0.08	0.03	0.13	0.03	0.18	0.05	0.16	*0.03*	0.17	0.03	6.01	0.83	0.30
G. sacculifer (unclean)	5–7	0.35	0.19	0.07	0.30	0.06	0.02	0.10	0.02	0.13	0.04	0.12	*0.02*	0.13	0.02	6.20	0.80	0.28
G. sacculifer (unclean)	10–12	0.39	0.27	0.08	0.37	0.09	0.03	0.12	0.02	0.17	0.04	0.14	*0.03*	0.15	0.03	5.86	0.88	0.34
G. sacculifer (unclean)	15–17	0.39	0.31	0.09	0.39	0.09	0.03	0.13	0.02	0.17	0.04	0.12	*0.02*	0.14	0.02	5.06	0.99	0.37
G. sacculifer (unclean)	19–21	0.50	0.37	0.11	0.49	0.13	0.04	0.16	0.03	0.21	0.05	0.14	*0.02*	0.15	0.02	4.55	1.06	0.36
G. sacculifer	0–2	0.28	0.16	0.05	0.20	0.04	0.01	0.06	0.01	0.09	0.02	0.08	*0.03*	0.08	0.01	6.08	0.72	0.33
G. sacculifer	5–7	0.32	0.18	0.05	0.24	0.04	0.01	0.07	0.01	0.11	0.02	0.09	*0.02*	0.09	0.01	5.92	0.72	0.31
G. sacculifer	10–12	0.24	0.13	0.04	0.18	0.03	0.01	0.05	0.01	0.08	0.02	0.07	*0.02*	0.07	0.01	6.08	0.71	0.32
G. sacculifer	15–17	0.26	0.18	0.05	0.21	0.04	0.01	0.06	0.01	0.11	0.02	0.08	*0.02*	0.09	0.01	6.04	0.74	0.37
G. sacculifer	19–21	0.26	0.19	0.05	0.22	0.05	0.01	0.06	0.01	0.10	0.02	0.08	*0.02*	0.08	0.01	5.42	0.84	0.40
Cibicidoides	0–2	0.44	0.17	0.07	0.33	0.06	0.02	0.08	0.01	0.11	0.03	0.09	*0.02*	0.09	0.02	4.27	0.84	0.22
Cibicidoides	5–7	0.74	0.29	0.12	0.52	0.09	0.03	0.14	0.02	0.18	0.04	0.14	*0.02*	0.14	0.03	4.09	0.90	0.22
Cibicidoides	10–12	0.52	0.25	0.09	0.38	0.07	0.02	0.10	0.02	0.14	0.03	0.11	*0.02*	0.11	0.02	4.24	0.87	0.26
Cibicidoides	15–17	0.70	0.35	0.12	0.49	0.09	0.03	0.14	0.02	0.18	0.04	0.14	*0.02*	0.14	0.02	4.19	0.89	0.28
Cibicidoides	19–21	0.72	0.39	0.12	0.50	0.09	0.03	0.15	0.02	0.19	0.04	0.15	*0.02*	0.14	0.02	4.43	0.89	0.30
Uvigerinidae	0–2	0.89	0.68	0.15	0.66	0.10	0.04	0.14	0.02	0.21	0.05	0.16	*0.04*	0.17	0.03	3.81	0.77	0.42
Uvigerinidae	5–7	0.79	0.47	0.13	0.60	0.10	0.04	0.13	0.02	0.20	0.05	0.16	*0.03*	0.16	0.02	4.12	0.80	0.33
Uvigerinidae	10–12	1.13	0.75	0.20	0.82	0.14	0.06	0.19	0.03	0.28	0.06	0.22	*0.04*	0.22	0.03	4.06	0.78	0.36
Uvigerinidae	15–17	0.93	0.54	0.16	0.65	0.12	0.04	0.14	0.02	0.23	0.05	0.17	*0.03*	0.18	0.03	3.91	0.74	0.32
Uvigerinidae	19–21	0.92	0.52	0.17	0.65	0.12	0.04	0.15	0.03	0.25	0.05	0.19	*0.03*	0.18	0.03	3.97	0.79	0.30

[a] Values are REE:Ca in μmol:mol.
[b] Tm is suspect, probably due to inter-REE molecular interference in the ICP-MS.
[c] HREE:LREE is defined as the ratio of shale normalized averaged Er:Ca, Yb:Ca to averaged Pr:Ca, Nd:Ca.
[d] MREE* is defined as average shale normalized (Gd:Ca, Tb:Ca) divided by average (Pr:Ca, Nd:Ca, Er:Ca, Yb:Ca).
[e] Ce* is defined by 2(Ce:Ca)/(La:Ca+Pr:Ca), when all values are shale normalized.

Because the diagenetic environment at 54MC is oxic, these foraminiferal shells are potentially coated with metal oxides. If Mn-oxides are not carriers of REEs (as discussed previously; [16]), any "metal oxide" influences on the REEs must be related to Fe-oxide cycling. To determine if the differences between HYDRX-cleaned and DIW-cleaned foraminifera described previously (Fig. 2) was consistent down core,

Table 6
Sta. 10 down core REE:Ca ratios

Species	Depth(cm)	La[a]	Ce	Pr	Nd	Sm	Eu	Gd	Tb	Dy	Ho	Er	Tm[b]	Yb	Lu	HREE[c] / LREE	MREE*[d]	Ce*[e]
Mixed planktonic	0–1	3.31	3.63	0.85	3.84	0.69	0.20	0.72	0.11	0.62	0.03	0.24	*0.01*	0.26	0.00	0.99	1.59	0.50
Mixed planktonic	5–7	5.39	17.60	1.74	7.09	1.37	0.37	1.37	0.23	1.31	0.22	0.67	*0.21*	0.47	0.09	1.16	1.53	1.30
Mixed planktonic	8–10	13.43	36.27	3.64	14.81	3.05	0.78	3.21	0.52	2.93	0.51	1.38	*0.18*	1.04	0.14	1.18	1.64	1.19
Mixed planktonic	20–22	7.97	19.03	2.22	8.64	1.87	0.54	1.97	0.36	2.13	0.38	1.11	*0.17*	0.95	0.13	1.70	1.46	1.04
Mixed planktonic	24–26	23.73	67.80	7.72	31.77	6.63	1.67	5.91	1.05	7.02	1.11	3.68	*0.50*	2.98	0.37	1.53	1.28	1.14
Uvigerinidae	0–1	6.34	10.35	1.75	6.95	1.35	0.33	1.36	0.21	1.17	0.19	0.54	*0.09*	0.43	0.05	1.00	1.54	0.71
Uvigerinidae	5–7	8.08	18.86	2.32	9.21	1.81	0.43	1.67	0.26	1.45	0.24	0.67	*0.09*	0.46	0.06	0.88	1.56	1.00
Uvigerinidae	8–10	15.45	37.96	4.42	17.16	3.41	0.84	3.37	0.54	2.97	0.48	1.29	*0.16*	0.91	0.12	0.91	1.65	1.05
Uvigerinidae	20–22	7.07	16.18	1.98	7.62	1.51	0.39	1.61	0.27	1.57	0.27	0.75	*0.10*	0.57	0.07	1.23	1.56	0.99
Uvigerinidae	24–26	5.58	12.69	1.54	6.20	1.22	0.32	1.34	0.22	1.27	0.23	0.64	*0.09*	0.52	0.07	1.35	1.51	0.99
Globobulimina	0–1	8.77	16.50	2.39	9.66	1.84	0.49	1.83	0.28	1.57	0.25	0.71	*0.11*	0.55	0.06	0.94	1.56	0.83
Globobulimina	5–7	6.23	16.30	1.75	6.94	1.36	0.33	1.31	0.21	1.11	0.19	0.54	*0.07*	0.38	0.05	0.95	1.56	1.13
Globobulimina	8–10	6.38	15.69	1.72	6.77	1.33	0.33	1.34	0.21	1.18	0.20	0.52	*0.07*	0.37	0.05	0.94	1.65	1.09
Globobulimina	20–22	4.24	9.86	1.21	4.59	0.92	0.24	0.98	0.17	0.96	0.17	0.47	*0.06*	0.36	0.05	1.28	1.53	1.00
Globobulimina	24–26	2.95	6.89	0.78	3.18	0.60	0.16	0.66	0.11	0.65	0.12	0.34	*0.05*	0.28	0.04	1.41	1.43	1.05

[a] Values are REE:Ca in μmol:mol.
[b] Tm is suspect, probably due to inter-REE molecular interference in the ICP-MS.
[c] HREE:LREE is defined as the ratio of shale normalized averaged Er:Ca, Yb:Ca to averaged Pr:Ca, Nd:Ca.
[d] MREE* is defined as average shale normalized (Gd:Ca, Tb:Ca) divided by average (Pr:Ca, Nd:Ca, Er:Ca, Yb:Ca).
[e] Ce* is defined by 2(Ce:Ca)/(La:Ca+Pr:Ca), when all values are shale normalized.

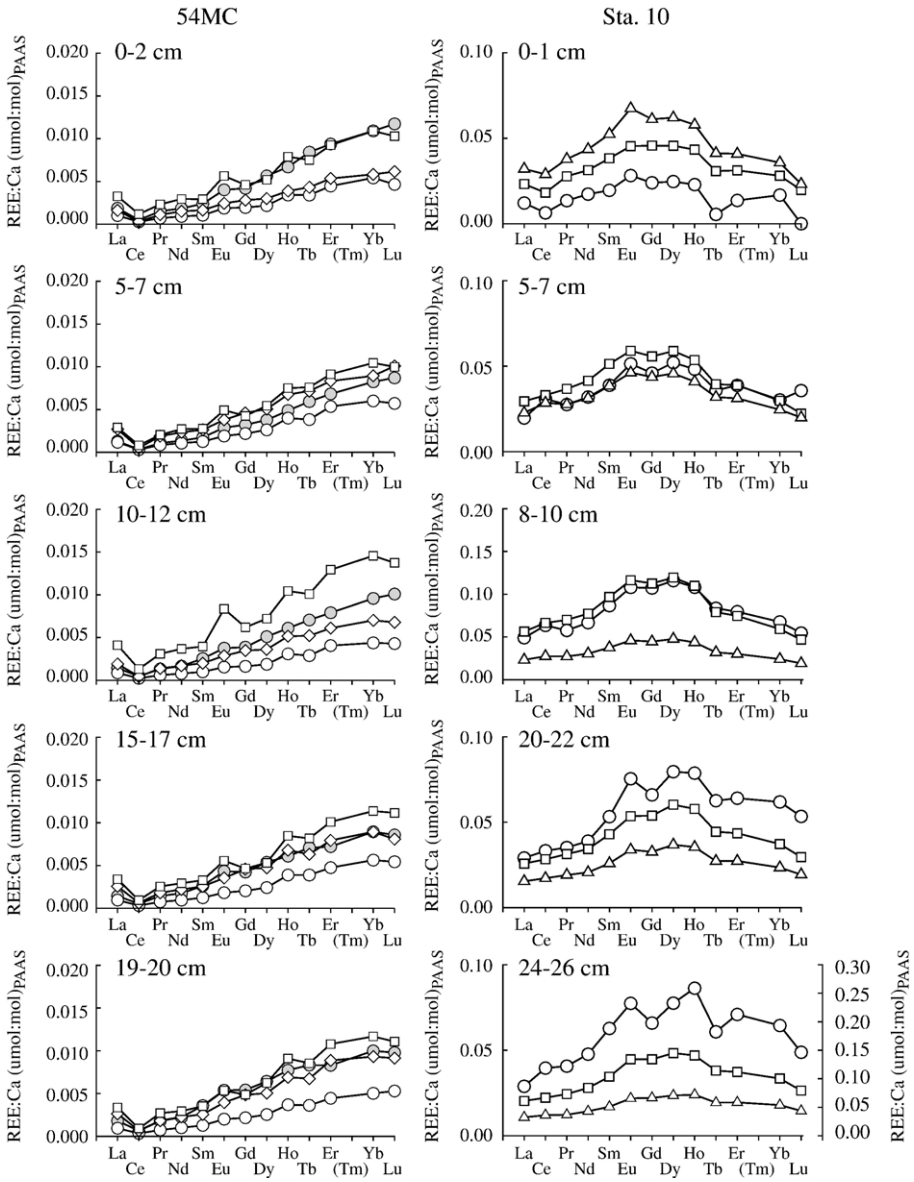

Fig. 6. Down core REE patterns. 54MC *G. sacculifers* (cleaned: empty ○; uncleaned: filled ●); *Cibicidoides* (◇) and *Uvigerinidae* (□) shown on left. Sta. 10 mixed planktonic (○); *Uvigerinidae* (□) and *Globobulimina* (Δ) shown on right. The mixed planktonic at 24–26 cm depth for Sta. 10 plots on the additional *y*-axis.

we ran a set of DIW-cleaned planktonics down core at this site. Again, and consistently, we found that the DIW-cleaned samples had higher REE : Ca ratios than those cleaned with HYDRX (Fig. 6). The patterns, however, are similar between each HYDRX–DIW-cleaned pair. The average HREE : LREE (5.5) of all the DIW-cleaned down core samples is similar to that of the HYDRX-cleaned samples (5.9), as are the "Ce anomalies" (0.33 average DIW-cleaned; 0.35 average HYDRX-cleaned; Table 5). Apart from the overall concentrations, the only possible difference is the MREE enrichment, which is more than 20% higher in the DIW-cleaned samples (0.91 DIW-cleaned average; 0.75 HYDRX-cleaned average). These observations allude to Fe-oxide contamination, but also imply that this contaminant phase has REEs virtually identical in pattern to the shell itself, and is probably a phase that forms coevally with calcification of the shell.

3.3.2. Sta. 10

The REE patterns of all the foraminifera, at every depth at Sta. 10 have a "MREE 352 bulge" type pattern

(Fig. 6). This suggests that under such intense diagenetic environments the primary foraminiferal REEs are overprinted by the pore water signal [16]. Indeed, the HREE:LREE, MREE* and Ce* values are similar between all the samples (~0.9 to 1.7, ~1.3 to 1.6 and >0.5, respectively). However, although the patterns are similar, the fact that REE concentrations are not equal is important for the REE paleoproxy. This is best demonstrated through comparison of the different foraminiferal REE concentrations to the REE pore water profiles at this site, as follows. The planktonic samples show increasing REE:Ca to the 8–10 cm sample; the 20–22 cm sample is slightly less concentrated; and the 24–26 cm sample is most concentrated (about an order-of-magnitude greater than the 0–2 cm sample; Table 6). The shallow infaunal *Uvigerindae* increase in REE concentration to the 8–10 cm sample and then REE concentrations decrease further down core. The deep infaunal *Globobuliminae* decrease in REE concentration with increasing depth (Table 6). These trends can be contrasted to the pore water REE profiles at Sta. 10, which show maxima at ~3 cm that diffuse to a sink at ~8 cm [16]. These pore water REE maxima are driven by Fe-oxide reduction, which occurs at the same depths [16] and is the source for the contaminant REEs measured on the foraminifera at Sta. 10. However, being anoxic, the contaminant phase cannot be Fe-oxide (or Mn-oxide, which is reduced prior to Fe in the diagenetic sequence; [53]). The fact that the contaminant phase dissolves readily in a stream of dilute acid, simultaneously with foraminiferal dissolution, suggests that the contaminant phase is rather mobile. As discussed previously, barite is unlikely the contaminant phase (i.e., it is immobile in a stream of weak acid [29,30]). Moreover, any environmental readsorption process is unlikely because we would expect to see similar down core REE:Ca trends for all three foraminiferal types if this were the case. Iron carbonate (siderite) seems to be the most likely source of the overprint. Siderite contamination is consistent with the fact that Fe:Ca measured in these samples is consistently high (>50 μmol:mol, and often above 100 μmol:mol). Furthermore, because the REE:Ca in the *Globobulimina* decrease constantly down core (Table 6) suggests that these shells are not prone to siderite contamination in the upper ~25 cm. That is, the *Globobulimina* shells "escape" diagenesis and might still hold promise as a paleoproxy.

In summary, these data indicate that the REE paleoproxy is applicable within oxic sedimentary environments, but not in sediments that have undergone anoxic diagenesis. Of course, if the diagnostic "MREE bulge" pattern is seen down core, especially in planktonic foraminifera, it can be assumed that those sediments have undergone anoxic conditions at some point in time, an observation that, in itself, could be useful for paleoceanographers (e.g., as an indicator of ocean anoxic events).

4. Discussion

Our main goal here is to evaluate the utility of the REEs as a paleoproxy. For this reason, this discussion will focus on the core top samples and how the REEs relate to paleoceanographically important parameters in the modern ocean. The down core sampling scheme was intended not for paleoceanographic purposes, but as a test of the influence of diagenesis, and, as discussed previously, we will not use these data to make any attempts at paleoceanographic reconstructions.

4.1. Core top samples

Two types of foraminifera were analyzed here: planktonics and benthics. These types reflect different life habitats and thus have different potential uses as paleoproxies. In all cases, Sta. 10 data will not be discussed, because the samples were apparently diagenetically altered (see Results section).

4.1.1. Planktonic foraminifera paleoproxy

The REEs in planktonic foraminifera were expected, a priori to have two possible uses as a paleoproxy: (1) The REE pattern was expected to reflect upper water column circulation, because of the relatively short residence time of REEs (<1000 y steady state whole ocean estimate; [17,33,41,42,52,54]), and the dominance of river/aeolian input to the upper water column ([54–57]). (2) The "Ce anomaly" has been hypothesized to reflect the oxygen content of seawater (higher O_2 content corresponding to higher "Ce anomaly;" e.g., [52], although this was foreseen as being more difficult to interpret [33,58,59]).

To avoid bias in light of these a priori notions, these REE data were compared to a more general compilation of a number of oceanic variables taken from World Ocean Atlas (WOA) [60] from grid points as close to the sites as possible ($T_{\text{in situ}}$; $T_{\text{pot.}}$; salinity; density; chlorophyll; nitrate; phosphate; silica; oxygen; Apparent Oxygen Utilization (AOU); and carbonate ion concentration). Satellite-based primary productivity estimates from the databases of Antoine et al. [61,62] were also compared to the REE data, again with grid points as close as possible to our sites. Cross-correlation matrices of

these data, as well as the latitude, longitude, La : Ca, HREE : LREE and Ce* of the samples were made for each of four depths: the sea surface; the mixed layer depth; the shallowest pycnocline; and the maximum pycnocline (the latter two to account for seasonal pycnoclines). These four depths represent the upper water column in which the planktonic foraminifera may live. The resulting correlation matrices were used to isolate the water column features best statistically correlated to the REE data. The closest fits are shown in Fig. 7.

These analyses indicate that two REE parameters will be useful paleoceanographic proxies (Fig. 7):

1. The La : Ca (the "REE concentration") of planktonic foraminifera are anticorrelated with annual primary production estimates (of course, oxygen, AOU and primary productivity are highly correlated in the subsurface waters analyzed, as discussed later).
2. The HREE : LREE of planktonic foraminifera correlates to water mass and good correlations were found with latitude, temperature, salinity and density (all of which are correlated in that they reflect "water mass").

The exception in both cases is the *G. sacculifer* samples from 54MC (Fig. 7). In terms of the first paleoproxy, this anomalous 54MC *G. sacculifer* sample might indicate that these foraminifera were not living in the same water mass as the other sites. That is, the sites 66MC, 64MC, 62MC, 50MC and 48MC represent a

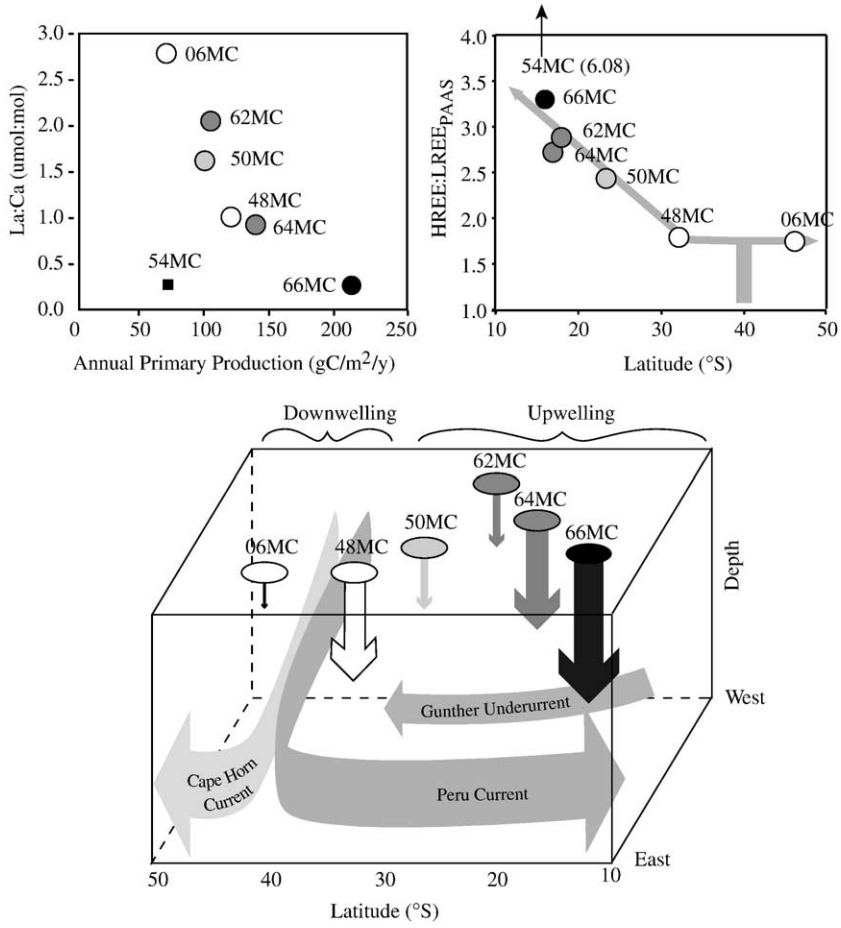

Fig. 7. Planktonic REE paleoproxy relationships. These relationships define the uses of the REE paleoproxy. 54MC appears as a flier in both cases (see text). Left-panel: La : Ca correlates well to primary production (from [61]). Right-panel: HREE : LREE (PAAS-normalized; [31]) correlates to water mass (shown as latitude), pointing towards use as a tracer of circulation. Gray arrows indicate evolution pathways of HREE : LREE predicted. Bottom-panel: schematic representation of the mechanics of the planktonic REE paleoproxy in the modern ocean. The shading intensity mirrors the evolution of the $HREE : LREE_{PAAS}$ as a function of flow north (if reflecting the Peru Current) or flow south (if reflecting the Gunther Undercurrent). The arrow size reflects annual primary production from [61]. These two REE proxies are mutually exclusive: for example, productivity at 48MC and 64MC are similar, thus the La : Ca are similar, but the $HREE : LREE_{PAAS}$ differ, reflecting difference in location of these two sites.

north–south transect near the coastal upwelling region, reflecting source water upwelled from the Gunther undercurrent (Fig. 1) as it progresses southward. This undercurrent, and the associated coastal upwelling, ceases around 42° S [63], and site 06MC is in an area of downwelling. Therefore, the data from 06MC should not continue the trend defined by the other sites, and, indeed, it has a HREE:LREE very similar to that of 48MC. 54MC, on the other hand, is more likely outside the influence of coastal upwelling and its source waters are most likely upwelling Antarctic Intermediate Water (AAIW). In fact, a K_D calculation using the 54MC planktonic foraminifera sample and the surface water data of German et al. [35] produces a flat-pattern of K_Ds across the series that range from ~150 to ~350 (similar to the benthic range), consistent with 54MC water being similar to AAIW.

The suggestion that HREE:LREE traces water mass evolution appears to be robust, from the arguments made above. A problem specific to the idea that these HREE:LREE data are tracing the Gunther undercurrent is that upwelling is restricted to a fairly narrow coastal zone along Chile [63], which might pose difficulties for interpreting the data from 50MC (and even 48MC) in this way. However, the HREE:LREE trend (Fig. 7) may, alternatively, be tracking the Peru Current northwards. This latter interpretation carries different implications, but does not change the general conclusion that the HREE:LREE in planktonic foraminifera can be used as a proxy of water mass.

The second planktonic REE proxy we suggest is that the REE concentrations reflect upper ocean biologic productivity. In this case, the 54MC data are more problematic. A possible explanation for this discrepancy is that La:Ca is a function of more than the one variable, just as oxygen isotopes are a function of both temperature and ice volume. Alternatively, the 54MC sample may simply not reflect modern seawater, due to the slow sedimentation rate at this site (1–5 cm/kyr; [64]). The measured oxygen-isotopic value of these samples ($\delta^{18}O = 0.17‰_{PDB} +/- 0.01$) suggests that this core top sample might reflect a mixture of Holocene foraminifera (with $\delta^{18}O = \sim -0.5‰_{PDB}$) and Last Glacial Maximum foraminifera (with $\delta^{18}O = \sim 1.0‰_{PDB}$).

Beyond the anomalous behavior of 54MC, the general relationships described above are satisfying because they agree with our predictions of the use of a REE paleoproxy, described now (Fig. 7). The overall REE pattern evolves with water mass age, (reflected in the HREE:LREE of the foraminifera), due to the short residence times and riverine/aeolian source of REEs to the surface oceans. Even as the pattern evolves, the amount of REE incorporated into the foraminiferal shells reflects surface ocean "biologic activity" (reflected in the La:Ca). Following recent observations, it is becoming clear that REEs are, to a great extent, controlled by organic carbon dynamics (see K_D discussion above, and [16,17,43–47,64]). (Indeed, the "Ce anomaly" is not likely a function of varying Ce – in a stable Ce(IV) solid state – but of La and Pr changes driven by organic processes [33,65].) Therefore, the lower La:Ca in regions of higher primary production would be due to the rapid removal of the REEs onto sinking particles, which will constitute a greater output flux under regions of high biological activity.

4.1.2. Benthic foraminifera paleoproxy

As a paleoproxy, the REEs in benthic foraminifera are far more straightforward. The REEs increase dramatically across the sediment–water interface, driven by remineralization of organic carbon that has survived water column degradation [16]. Because of this, the differences in REE content between the shallow infaunal *Uvigerinidae* and the epifaunal *Cibicidoides* should reflect organic carbon flux to the sea floor, as the results indicate (Fig. 8).

Of course, surface seawater productivity is unlikely to be the cardinal variable for this paleoproxy as suggested in Fig. 8. More exactly, it is the carbon flux at the sediment–water interface that controls this $REE_{Cibicidoides}:REE_{Uvigerinidae}$ relationship. Because these sites all have depth >1000 m and bottom water oxygen >100 μM, the extent of water column remineralization is likely comparable [66]. Therefore, the seafloor flux of organic carbon should mirror surface seawater productivity. However, for future

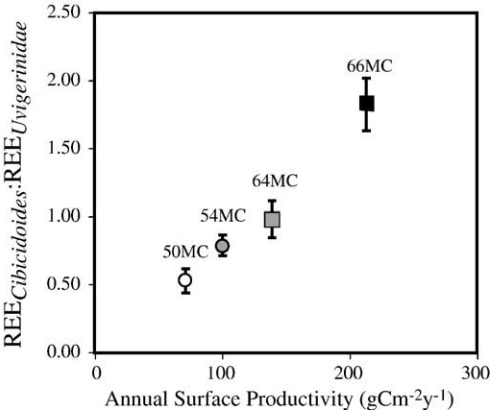

Fig. 8. The mean and standard deviation (error bars) of all 13 epifaunal:infaunal REE-ratios at the four sites plotted against surface ocean productivity (from [61]).

paleoproxy application, a more rigorous assessment of how water column remineralization factors in needs to be done (perhaps even through use of the planktonic foraminiferal REE signal).

Finally, we have three values for REEs in deep-infaunal benthic foraminifera from coretop samples (Table 4). Although too few samples to delimit paleoproxy potential, two observations are noteworthy: first, there is obviously a dynamic signal in these foraminifera (Fig. 5). Indeed, finding the cause of the surprisingly low REE:Ca in the 39MC samples, a deeply anoxic site, may help explain the low Nd concentrations found in foraminifera from Mediterranean saporopels [21]. Second, the fact that the REE:Ca ratio in these foraminiferal shells does not reflect the down core trends of the planktonic and shallow infaunal foraminifera (at Sta. 10) suggests that this signal is primary, and potentially worth further investigation as a paleoproxy.

5. Conclusions

The goal of this work was to determine the utility of the rare earth elements in foraminiferal calcite as a paleoproxy. These results show that planktonic and benthic foraminiferal REEs can be used for reconstructing surface water circulation and productivity, and organic carbon flux to the seafloor, respectively. Thus, the REE paleoproxy of these oceanographically important variables will prove greatly beneficial for paleoceanographic studies.

Beyond these conclusions, we have made several important observations and speculations about REEs and foraminifera. These are:

- Flow-through cleaning and dissolution can successfully isolate primary foraminiferal calcite, although it has yet to be determined if siderite can be isolated from calcite in this system. Furthermore, although DTPA-cleaning is not necessary due to the non-aggressive FT dissolution protocols, it appears that HYDRX-cleaning removes a source of contaminant REEs. However, the use of HYDRX-cleaning must be tempered by the fact that it remobilizes metal-oxides that are otherwise immobile with a simple DIW-rinse of the sample.
- A simple readsorption model is used to demonstrate that readsorption is an important property of REEs and should be taken into consideration during any laboratory process involving REEs.
- The distribution coefficients of REEs in foraminiferal calcite are between 100 and 500. Although higher than any other K_D yet found in foraminiferal calcite, such high K_Ds should be considered reasonable, as suggested by our proposed biochemical mechanism.
- Intense diagenetic environments preclude the use of a REE paleoproxy, although such conditions will be clear in any paleo-record and thus can be recognized. This observation itself could lend itself to paleoceanographic interpretations.

Acknowledgements

All credit to Andy Ungerer, manager of the W.M. Keck Collaboratory for Plasma Spectrometry, for his ageless help. June Wilson, Bill Rugh and all the third floor foram group were crucial in all the foram picking and oxygen analyses. BAH cannot construct the sentence to thank Delphine Haley. Conversations with Fred Prahl and Bob Collier were, and always are, enlightening. Special thanks to Ed Boyle for his editorial handling, and three anonymous reviewers whose comments improved this manuscript considerably. This work was supported by NSF grants OCE-9986399 and OCE-0136905 to GPK and ACM, and the generosity of the W.M. Keck Foundation.

Appendix A. Readsorption model

The readsorption model is described as follows:

For each time slice (n; equivalent to the fraction collected) and each REE (m), a value of $REE_{(n,m)}$ is made using the following equation:

$$REE_{(n,m)} = \left\{ \left(\frac{REE_{(n-1,m)}}{[Ca]_{(n-1)}} \right) \times [Ca]_{(n)} \right\} + \left\{ \left(\frac{REE_{(n-1,m)}}{[Ca]_{(n-1)}} \right) \times Ca_n \times RFX \right\}$$

where:

- $(n-1)$ when $n=1$ is an "initial guess" of REE (m) (i.e., $REE_{(0,m)}$. This is the solution for the primary REE signal in the foraminifera. Initially, this is set at 1 for all $REE_{(0,m)}$ in these runs);
- [Ca]=total amount of calcium left as a solid (undissolved);
- Ca=concentration of calcium measured at a given time slice, such that $\Sigma Ca=[Ca]_0$, and;
- RFX="readsorption factor;" a value between 0 and 1, where 1=100% readsorption. For the data modeled, RF1 (the readsorption factor assigned to the

weak acid) averaged ~0.4 (40%), RF2 (the readsorption factor assigned to the strong acid) averaged ~0.05 (5%).

Simultaneously, the REE : Ca model ratio is made for each time slice using the equation:

$$\mathrm{REE:Ca}_{(n,m)} = \frac{\left\{\mathrm{REE}_{(n-1,m)}/[\mathrm{Ca}]_{n-1} \times \mathrm{Ca}_n \times (1-\mathrm{RFX})\right\}}{\mathrm{Ca}_n}.$$

The model then iterates on the initial value of $\mathrm{REE}_{(0,m)}$ 20 times, which is usually more than sufficient to reach a stable result. Each iteration corrects the $\mathrm{REE}_{(0,m)}$ through half the difference of the model predicted REE : Ca and the measured REE : Ca of the fraction collected that had the highest measured calcium concentration. This value was used as a goal for the model because it represents both a large signal for detection (i.e., highest measurement confidence) and a point in the dissolution where readsorption is least likely.

References

[1] D.W. Lea, Constraints on the alkalinity and circulation of glacial circumpolar deep water from benthic foraminiferal barium, Glob. Biogeochem. Cycles 7 (1993) 695–710.

[2] A.D. Russell, S. Emerson, B.K. Nelson, J. Erez, D.W. Lea, Uranium in foraminiferal calcite as a recorder of seawater uranium concentrations, Geochim. Cosmochim. Acta 58 (1994) 671–681.

[3] D.W. Hastings, S.R. Emerson, J. Erez, B.K. Nelson, Vanadium in foraminiferal calcite: evaluation of a method to determine paleo-seawater vanadium concentrations, Geochim. Cosmochim. Acta 60 (1996) 3701–3715.

[4] M.R. Palmer, P.N. Pearson, S.J. Cobb, Reconstructing past ocean pH-depth profiles, Science 282 (1998) 1468–1471.

[5] H. Elderfield, R.E.M. Rickaby, Oceanic Cd/P ratio and nutrient utilization in the glacial southern Ocean, Nature 405 (2000) 305–310.

[6] C. Pomies, G.R. Davies, S.M.-H. Conan, Neodymium in modern foraminifera from the Indian Ocean: implications for the use of foraminiferal Nd isotope compositions in paleo-oceanography, Earth Planet. Sci. Lett. 203 (2002) 1031–1045.

[7] A.L. Cohen, K.E. Owens, G.D. Layne, N. Shimizu, The effect of algal symbionts on the accuracy of Sr/Ca paleotemperatures from coral, Science 296 (2002) 331–333.

[8] P.S. Dekens, D.W. Lea, D.K. Pak, H.J. Spero, Core top calibration of Mg/Ca in tropical foraminifera: refining paleotemperature estimation, Geochem. Geophys. Geosyst. 3 (2002) (2001GC000200 [14,630 words]).

[9] C. Siebert, T.F. Nagler, F. van Blankenburg, J.D. Kramers, Molybdenum isotope records as a potential new proxy for paleoceanography, Earth Planet. Sci. Lett. 211 (2003) 159–171.

[10] C.H. Lear, H. Elderfield, P.A. Wilson, A Cenozoic seawater Sr/Ca record from benthic foraminiferal calcite and its application in determining global weathering fluxes, Earth Planet. Sci. Lett. 208 (2003) 69–84.

[11] S. Pichat, C. Douchet, F. Albarede, Zinc isotope variations in deep-sea carbonates from the eastern equatorial Pacific over the last 175 ka, Earth Planet. Sci. Lett. 210 (2003) 167–178.

[12] M. Palmer, Rare earth elements in foraminiferal tests, Earth Planet. Sci. Lett. 73 (1985) 285–298.

[13] E.A. Boyle, Cadmium, zinc, copper, and barium in foraminiferal tests, Earth Planet. Sci. Lett. 53 (1981) 11–35.

[14] E. Sholkovitz, Artifacts associated with the chemical leaching of sediments for rare-earth elements, Chem. Geol. 77 (1989) 47–51.

[15] B. Haley, G.P. Klinkhammer, Development of a flow-through system for cleaning and dissolving foraminiferal tests, Chem. Geol. 185 (2002) 51–69.

[16] B.A. Haley, G.P. Klinkhammer, J. McManus, Rare earth elements in pore water of marine sediments, Geochim. Cosmochim. Acta 68 (2004) 1265–1279.

[17] R.H. Byrne, E.R. Sholkovitz, Marine chemistry and geochemistry of the lanthanides, in: K.A. Gschneider Jr., L. Eyring (Eds.), The Handbook on the Physics and Chemistry of the Rare Earths, vol. 23, Elsevier Science B.V, Amsterdam, 1996, pp. 497–593.

[18] S. Barker, M. Greaves, H. Elderfield, A study of cleaning procedures used for Mg/Ca paleothermometry, Geochem. Geophys. Geosyst. 4 (2003) (2003GC000559 [9070 words]).

[19] G.P. Klinkhammer, B.A. Haley, A.C. Mix, H.M. Benway, M. Cheseby, Evaluation of automated flow-through time-resolved analysis of foraminifera for Mg/Ca paleothermometry, Paleoceanography 19 (2004), doi:10.1029/2004PA001050.

[20] D.W. Lea, E.A. Boyle, Determination of carbonate-bound barium in foraminifera and corals by isotope dilution plasma-mass spectrometry, Chem. Geol. 103 (1993) 73–84.

[21] D. Vance, A. Scrivner, P. Beney, M. Staubwasser, G.M. Henderson, N.C. Slowy, The use of foraminifera as a record of the past neodymium isotope composition of seawater, Paleoceanography 19 (2004), doi:10.1029/2003PA000957.

[22] A.W.H. Be, J.W. Morse, S.W. Harrison, Progressive dissolution and ultrastructural breakdown in planktonic foraminifera, in: W.V. Sliter, A.W.H. Be, W.H. Berger (Eds.), Dissolution of Deep-Sea Carbonates, vol. 13, Cushman Found. for Foraminiferal Res., Wash. D.C., 1975, pp. 27–55.

[23] A.W.H. Be, An ecological, zoogeographic and taxonomic review of recent planktonic foraminifera, in: A.T.S. Ramsay (Ed.), Oceanic Micropaleontology I, vol 1, Academic Press, London, 1977, pp. 1–100.

[24] M.L. Bender, R.B. Lorens, D.F. Williams, Sodium, magnesium and strontium in the tests of planktonic foraminifera, Micropaleontology 21 (1975) 448–459.

[25] S.J. Brown, H. Elderfield, Variations in Mg/Ca and Sr/Ca ratios of planktonic foraminifera caused by post depositional dissolution: evidence of shallow Mg-dependant dissolution, Paleoceanography 11 (1996) 543–551.

[26] D. Nurnberg, J. Bijma, C. Hembleben, Assessing the reliability of magnesium in foraminiferal calcite as a proxy for water mass temperatures, Geochim. Cosmochim. Acta 60 (1996) 803–814.

[27] H.M. Benway, B.A. Haley, G.P. Klinkhammer, A.C. Mix, Adaptation of a flow-through leaching procedure for Mg/Ca paleothermometry, Geochem. Geophys. Geosyst. 4 (2003) (2002GC00312 [6947 words]).

[28] E. Sholkovitz, T.J. Shaw, D.L. Schneider, The geochemistry of rare earth elements in the seasonally anoxic water column and porewaters of Chesapeake Bay, Geochim. Cosmochim. Acta 56 (1992) 3389–3402.

[29] E.E. Martin, J.D. MacDougall, T.D. Herbert, A. Paytan, M. Kastner, Strontium and neodymium isotopic analyses of marine barite separates, Geochim. Cosmochim. Acta 59 (1995) 1353–1361.
[30] K.B. Averyt, A. Paytan, G. Li, A precise, high-throughput method for determining Sr/Ca, Sr/Ba, and Ca/Ba ratios in marine barite, Geochem. Geophys. Geosyst. 4 (2003) (2002GC000467 [4833 words]).
[31] S.R. Taylor, S.M. McLennon, The Continental Crust: Its Composition and Evolution, Blackwell, Oxford, 1985, 312 pp.
[32] P.L. Verplanck, D.K. Nordstrom, H.E. Taylor, Overview of rare earth element investigations in acid waters of U.S. geologic survey abandoned mine lands, U.S. Geol. Surv. Water-Res. Inv. Rep. 99-4018A, vol. 1, 1999, pp. 83–93.
[33] B.A. Haley, G.P. Klinkhammer, Complete separation of rare earth elements from small volume seawater samples by automated ion chromatography: method development and application to benthic flux, Mar. Chem. 82 (2003) 197–220.
[34] M.R. Palmer, H. Elderfield, Rare earth elements and neodymium isotopes in ferromanganese oxide coatings of Cenozoic foraminifera from the Atlantic Ocean, Geochim. Cosmochim. Acta 50 (1986) 409–417.
[35] C.R. German, T. Masuzawa, M.J. Greaves, H. Elderfield, J.M. Edmond, Dissolved rare earth elements in the southern Ocean: cerium oxidation and the influence of hydrography, Geochim. Cosmochim. Acta 59 (1995) 1551–1558.
[36] L.D. Talley, Distribution and formation of north pacific intermediate water, J. Phys. Oceanogr. 23 (1993) 517–537.
[37] D.J. Piepgras, S.B. Jacobsen, The behavior of rare earth elements in seawater: precise determination of variations in the North Pacific water column, Geochim. Cosmochim. Acta 56 (1992) 1851–1862.
[38] D. Vance, K.W. Burton, Neodymium isotopes in planktonic foraminifera: a record of the response of continental weathering and ocean circulation rates to climate change, Earth Planet. Sci. Lett. 173 (1999) 365–379.
[39] K.W. Burton, D. Vance, Glacial-interglacial variations in the neodymium isotope composition of seawater in the Bay of Bengal recorded by planktonic foraminifera, Earth Planet. Sci. Lett. 176 (2000) 425–441.
[40] L.Z. Lakshtanov, S.L. Stipp, Experimental study of europium (III) coprecipitation with calcite, Geochim. Cosmochim. Acta 68 (2004) 819–827.
[41] E.D. Goldberg, M. Koide, R.A. Schmitt, R.H. Smith, Rare-earth distribution in the marine environment, J. Geophys. Res. 68 (1963) 4209–4217.
[42] H. Elderfield, M.J. Greaves, The rare earth elements in seawater, Nature 296 (1982) 214–219.
[43] J.K. Stanley Jr., R.H. Byrne, The influence of solution chemistry on REE uptake by *Ulva lactuaca* L. in seawater, Geochim. Cosmochim. Acta 54 (1990) 1587–1596.
[44] E.R. Sholkovitz, Chemical evolution of rare earth elements: fractionation between colloidal and solution phases of filtered river water, Earth Planet. Sci. Lett. 114 (1992) 77–84.
[45] R.H. Byrne, K.-H. Kim, Rare earth elements scavenging in seawater, Geochim. Cosmochim. Acta 54 (1990) 2645–2656.
[46] R. Arraes-Mescoff, M. Roy-Barman, L. Coppola, M. Souhaut, K. Tachikawa, C. Jeandel, R. Sempere, C. Yoro, The behavior of Al, Mn, Ba, Sr, REE and Th isotopes during in vitro degradation of large marine particles, Mar. Chem. 73 (2001) 1–19.
[47] J. Tang, K.H. Johannesson, Speciation of rare earth elements in natural terrestrial waters: assessing the role of dissolved organic matter from the modeling approach, Geochim. Cosmochim. Acta 67 (2003) 2321–2339.
[48] J.S. Evans, Principles of molecular biology and biomacromolecular chemistry, in: P.M. Dove, J.J. de Yoreo, S. Weiner (Eds.), Biomineralization, vol. 54, 2003, pp. 31–56.
[49] D.W. Lea, Trace elements in foraminiferal calcite, in: Sen Gupta (Ed.), Modern Foraminifera, Kluwer Academic Publishers, Dorrecht, 1999, pp. 259–277.
[50] A.E. Martell, R.M. Smith, Critical Stability Constants. Volume 1: Amino Acids, Plenum Press, New York, 1974.
[51] J.M. Bernhard, J.K. Blanks, C.J. Hintz, G.T. Chandler, T.J. Shaw, D.C. McCorkle, Sub-millimeter life positions and microhabitats of paleoceanographically-relevant benthic foraminifers: implications for paleoproxy interpretations, Eos Trans. AGU 84 (2003) (Ocean Sci. Meet. Suppl., Abstract OS42-02).
[52] H. Elderfield, The oceanic chemistry of rare earth elements, Philos. Trans. R. Soc. Lond. 325 (1988) 105–126.
[53] P.N. Froelich, G.P. Klinkhammer, M.L. Bender, N.A. Luedtke, G.R. Heath, D. Cullen, P. Dauphin, D. Hammond, B. Hartman, V. Maynard, Early oxidation of organic matter in pelagic sediments of the eastern equatorial Atlantic: suboxic diagenesis, Geochim. Cosmochim. Acta 43 (1979) 971–991.
[54] C.J. Bertram, H. Elderfield, The geochemical balance of the rare earth elements and neodymium isotopes in the oceans, Geochim. Cosmochim. Acta 57 (1993) 1957–1986.
[55] H. Elderfield, E.R. Sholkovitz, Rare earth elements in the pore waters of reducing nearshore sediments, Earth Planet. Sci. Lett. 82 (1987) 280–288.
[56] S.J. Goldstein, S.B. Jacobsen, The Nd and Sr isotopic sysematics of river-water dissolved material: implications for the sources of Nd and Sr in seawater, Chem. Geol. 66 (1987) 245–272.
[57] H. Elderfield, R. Upstill-Goddard, E.R. Sholkovitz, The rare earth elements in rivers, estuaries, and coastal seas and their significance to the composition of ocean waters, Geochim. Cosmochim. Acta 54 (1990) 971–991.
[58] C.R. German, H. Elderfield, Application of the Ce anomaly as a paleoredox indicator: the ground rules, Paleoceanography 5 (1990) 823–833.
[59] Y. Nozaki, D.-S. Alibo, H. Amakawa, T. Gamo, H. Hasumoto, Dissolved rare earth elements and hydrography in the Sulu Sea, Geochim. Cosmochim. Acta 63 (1999) 2171–2181.
[60] M.E. Conkright, R.A. Locarnini, H.E. Garcia, T.D. O'Brein, T.P. Boyer, C. Stephens, J.I. Antonov, World Ocean Atlas 2001: Objective Analyses, Data Statistics, and Figures, CD-ROM Documentation, National Oceanographic Data Center, Silver Spring, MD., 2002, pp. 1–17.
[61] D. Antoine, J.-M. Andre, A. Morel, Oceanic primary production 2. Estimation at global scale from satellite (coastal zone color scanner) chlorophyll, Glob. Biogeochem. Cycles 10 (1996) 57–69.
[62] D. Antoine, A. Morel, Oceanic primary production 1. Adaptation of a spectral light-photosynthesis model in view of application to satellite chlorophyll observations, Glob. Biogeochem. Cycles 10 (1996) 43–55.
[63] P.T. Strub, J.M. Mesias, V. Montecino, J. Rutllant, S. Salinas, Coastal Ocean Circulation off Western South America, in: A.R. Robinson, K.H. Brink (Eds.), The Sea, vol. 11, John Wiley and Sons, 1998, pp. 273–313.
[64] T. Tosiani, M. Loubet, J. Viers, M. Valladon, J. Tapia, S. Marrero, A. Yanes, A. Ramirez, B. Dupre, Major and race elements in river-borne materials from the Cuyuni basin (south-

ern Venezuela): evidence for organo-colloidal control on the dissolved load and element redistribution between the suspended and dissolved load, Chem. Geol. 211 (2004) 305–334.
[65] K. Tachikawa, M. Roy-Barman, A. Michard, D. Thouron, D. Yeghicheyan, C. Jeandel, Neodymium isotopes in the Mediterranean sea: comparison between seawater and sediment signals, Geochim. Cosmochim. Acta 68 (2004) 3095–3106.
[66] E. Suess, Particulate organic carbon flux in the oceans; surface productivity and oxygen utilization, Nature 288 (1980) 260–263.

View publication stats